1

2

3

Protocol-dependence of middle cerebral artery dilation to modest hypercapnia

6

7

Baraa K. Al-Khazraji[1], Sagar Buch[3], Mason Kadem[4], Brad J. Matushewski[2], Kambiz Norozi[5,8],

Ravi S. Menon[3,6], and J. Kevin Shoemaker[2,7]

10

11

[1]Department of Kinesiology, Faculty of Science, McMaster University, Hamilton, ON;

[2]School of Kinesiology, Faculty of Health Sciences;

[3]Centre for Functional and Metabolic Mapping, Robarts Research Institute;

[4]School of Biomedical Engineering, McMaster University, Hamilton, ON;

[5]Department of Pediatrics, [6]Department of Medical Biophysics, [7]Department of

Physiology and Pharmacology, Schulich School of Medicine and Dentistry, Western University,

London, ON

[8]Department of Pediatric Cardiology, Medical School Hannover, Germany

20

21

22

Correspondence

J. Kevin Shoemaker, PhD

The University of Western Ontario, London, Ontario, Canada, N6A 5K7

Email: kshoemak@uwo.ca

Phone: 519-661-2111, ext: 88157

Middle cerebral artery responses to vasoreactivity protocols

28   **Abstract**

29   There is a need for improved understanding of how different cerebrovascular reactivity (CVR)

30   protocols affect vascular cross-sectional area (CSA) when measures of vascular CSA are not

31   feasible. In human participants, we delivered $\sim\pm4mmHg$ end-tidal partial pressure of CO_2

32   ($PETCO_2$) relative to baseline through controlled delivery, and measured changes in middle

33   cerebral artery (MCA) cross-sectional area (CSA; magnetic resonance imaging (7 Tesla MRI)),

34   blood velocity (transcranial Doppler and Phase contrast MRI), and calculated CVR based on

35   steady-state versus a ramp protocol during two protocols: a 3-minute steady-state (+4mmHg

36    $PETCO_2$) and a ramp (delta of -3 to +4mmHg of $PETCO_2$). We observed that 1) the MCA did not

37   dilate during the ramp protocol, but did dilate during steady-state hypercapnia, and 2) MCA blood

38   velocity CVR was similar between ramp and steady-state hypercapnia protocols, although

39   calculated MCA blood flow CVR was greater during steady-state hypercapnia than during ramp,

40   the discrepancy due to MCA CSA changes during steady-state hypercapnia. Due to the ability to

41   achieve similar levels of MCA blood velocity CVR as steady-state hypercapnia, the lack of change

42   in MCA cross-sectional area, and the minimal expected change in blood pressure, we propose that

43   a ramp model, across a delta of $\sim$-3 to +4mmHg $PETCO_2$, may provide one alternative approach

44   to collecting CVR measures in young adults with TCD when CSA measures are not feasible.

45

46   **Keywords**

49

50   **Running Title**

51   Middle cerebral artery responses to vasoreactivity protocols

Introduction

52 Cerebrovascular reactivity (CVR) studies assess changes in cerebral blood flow to a known

53 vasoreactive stimulus (e.g., changes in end-tidal partial pressure of CO_2; PETCO$_2$). Measures of

54 CVR are important because attenuated CVR may reflect preclinical vascular pathophysiology and

55 an increased risk of mortality independent from cardiovascular risk factors or stroke incidence [1].

56 The most commonly used technique for CVR measures in humans, transcranial Doppler (TCD)

57 ultrasonography, provides an index of vascular blood flow changes (i.e., blood velocity) because

58 the vascular cross-sectional area (CSA) values required for blood flow calculations (i.e., the

59 product of CSA and blood velocity) are not collected with TCD. Thus, an assumption of an

60 unchanging CSA is typically accepted, raising concern if changes in CSA do occur [2]. To

61 circumvent issues related to TCD measures of CVR, some research groups measure all four brain-

62 supply (i.e., carotid and vertebral) arteries outside of the brain [3], or use expensive neuroimaging

63 approaches [4,5].

65 An additional concern regarding quantification of CVR is the potential for changes in central

66 hemodynamics during hypercapnia (elevated PETCO$_2$) that could elevate cerebral blood flow due

67 to changes in cardiac output [6] and blood pressure [6,7] and not directly due to cerebrovascular

68 dilation [7]. Another complicating factor in quantifying CVR between groups is potential variation

69 in large cerebral artery reactivity, particularly when comparing age differences [8]. As an example,

70 our group's previous work showed that compared to younger adults, older adults exhibited

71 attenuated changes in large cerebral artery CSA in response to steady-state hypercapnia [9].

72 However, obtaining cerebral artery CSA data requires access to costly MRI or CT systems. We

73 aim to understand protocol designs that provide accurate CVR estimates when using TCD

74 methods. The "*ideal*" velocity based CVR protocols conducted using TCD would require: 1)

75 minimal CSA changes by conducting CVR protocols that result in negligible change in CSA, and

76 2) minimal influence of confounding variables such as blood pressure.

77 In the current study, we tested the hypothesis that a ramp (i.e., linear) CVR protocol within the ±5

78 mmHg range of relative changes in PETCO$_2$ would provide minimal changes in CSA while still

79 replicating CVR outcomes from the more standard steady-state hypercapnia CVR protocol. Our

80 rationale for this range of relative changes in PETCO$_2$ comes from the emerging knowledge of a

81 sigmoidal change in MCA CSA, with minimal changes in hypercapnia, within the -5 to +5 mmHg

82   from resting PETCO$_2$ (10). We chose a ramp-style CVR protocol to compare to CVR measures

83   from a steady-state hypercapnia protocol (0 to ~5 mmHg) because: 1) the ramp protocol is a well-

84   established protocol for CVR measures (7,11,12), and 2) existing means for calculating CVR from

85   standard steady-state protocols use linear slope methods which simply reduce to a ramp design.

86   We acknowledge that the ramp protocol within the ~$\Delta\pm5$ mmHg from baseline PETCO$_2$ range may

87   potentially affect vascular dilation differently than a steady-state hypercapnia protocol as the

88   hypocapnia portion preceding hypercapnia may blunt blood velocity CVR (13). A sub-analysis in

89   our earlier work, however, indicated that order of condition did not affect CSA reactivity in young

90   adults (4). Additionally, existing methods primarily focus on velocity-based CVR without

91   considering CSA, and we wanted to design a CVR protocol that minimized CSA changes (even if

92   it involved hypocapnia) and blood pressure changes while retaining its ability to elevate cerebral

93   blood flow (i.e., changing blood velocity). Other models can be considered but we want to test the

94   ramp protocol as one example of alternative CVR designs that may elicit negligible CSA and BP

95   changes when measuring blood velocity CVR using TCD.

96   To achieve the high temporal resolution of the MCA CSA for the required study, we developed a

97   dynamic anatomical imaging sequence with high-temporal and spatial resolution to capture MCA

98   CSA changes every 14 seconds throughout each vasoreactivity protocol (~$\pm\Delta4$ mmHg) using 7T

99   magnetic resonance imaging. Our objectives were to assess whether between steady-state and ramp

100   protocols: 1) the MCA CSA increased compared to baseline, 2) blood pressure remained stable

101   throughout duration of the protocol, and 3) MCA blood velocity (via TCD alone), and calculated

102   flow vasoreactivity were similar.

Materials and Methods

Participants

105   All testing was conducted at the Centre for Functional and Metabolic Mapping at The University

106   of Western Ontario. The Human Subjects Research Ethics Board at the University of Western

107   Ontario (London, Ontario, Canada) approved the experiment protocols herein. Informed consent

108   from 12 healthy subjects (19-25 years of age; 6 males) was obtained prior to scanning. A sample

109   size calculation was based off of our previous work with blood velocity reactivity measured with

110   TCD during steady-state hypercapnia (4). Specifically, for a within-subject design, with a Cohen's

111   d of 1.02, alpha level of significance of 0.05, and statistical power of 0.80, we calculated a sample

112   size of 10 and recruited 12 individuals due to our laboratory's expected attrition rate of 10-12%

113   with our neuroimaging studies. Participants were ineligible if they were smokers, pregnant, or had

114   any of the following conditions: Raynaud's disease, respiratory illnesses, diabetes, claustrophobia,

115   history of psychosis, eating disorders, manic or bipolar disorder, major psychiatric conditions, or

116   dependence on alcohol or drugs.

Procedure and data recording

118   Testing was completed between 10am – 2pm. Participants refrained from exercise, alcohol, drugs,

119   and caffeine within 12 hours prior to testing. We used TCD and MRI to assess the cerebral

120   vasoreactivity in response to steady-state (three minutes) bouts of hypercapnia (HC), and a ramp

121   protocol from hypocapnia to hypercapnia (four minutes) (Fig. 1).
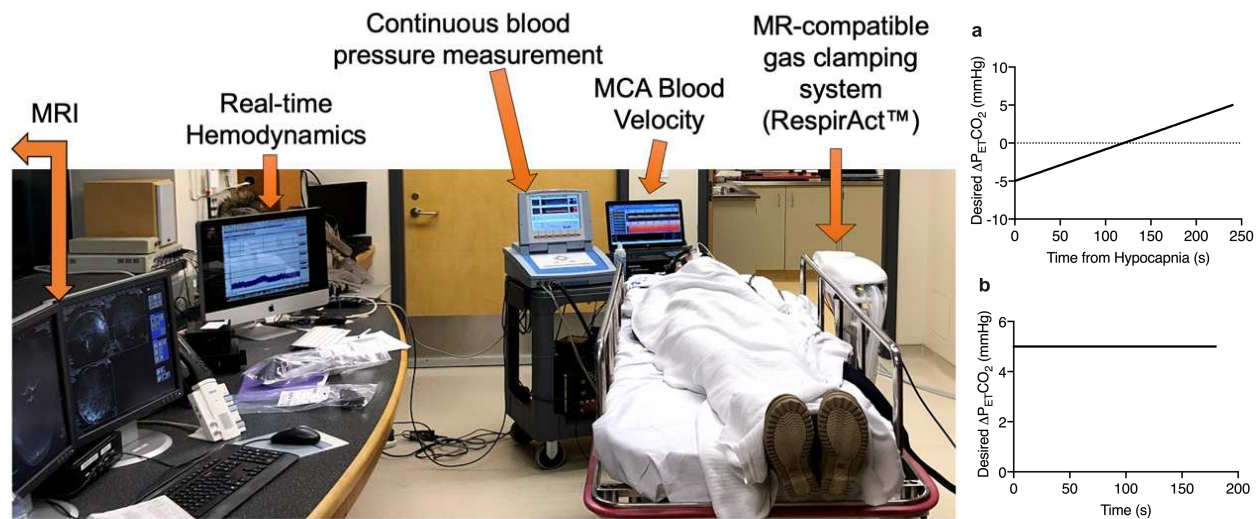

Figure 1 – Experimental protocol schematic. Left: Experimental setup displaying real-time data collection for both transcranial Doppler and MRI sessions. Right, panel a: Ramp hypercapnia protocol with a desired target range of -5 to +5 mmHg from baseline $PETCO_2$ and a duration of 240 seconds. Right, panel b: Steady-state hypercapnia (SSHC) protocol with a target range of +5 mmHg from baseline $PETCO_2$ and a duration of 180 seconds. Protocols were executed using the RespirAct™ device with preset protocols programmed with the desired $PETCO_2$ values.

122   Steady-state and ramp protocols were each conducted twice, once for each of the TCD and MRI

123   portions of the testing sessions and the order of TCD and MRI trials was randomized across

124   participants. Unfortunately, we were unable to randomize the order of CVR protocols as it was

125   difficult to stop and restart the RespirAct™ (Thornhill Research Inc., Toronto, Ontario, Canada)

126 without doing extensive recalibration. The desired ventilatory rate was set to 12 breaths/min using
127 a visual metronome for each session and was projected on a screen during the MRI scan. Our goal
128 was to have the protocols fall within the ±5 mmHg from baseline $PETCO_2$ range. Following a
129 familiarization period of four minutes, the order and duration of protocols occurred as follows: 1)
130 baseline (1 minute), 2) steady-state hypercapnia (target was +5 mmHg, although only reached
131 ~+4mmHg; three minutes), 3) recovery (2 minutes) 4) baseline (1 minute), 5) -5 mmHg $PETCO_2$
132 hypocapnia (brief hyperventilation; target was +5mmHg, although only reached ~ -3mmHg) 30
133 seconds), 6) incremental increase (ramp) from ~ -3 mmHg hypocapnia to ~ +4 mmHg relative
134 $PETCO_2$ hypercapnia (four minutes), 7) recovery (two minutes).

Manipulating target $PETCO_2$ stimulus

136 Prior to the MRI scan, participants were fitted with a facemask attached to the RespirAct™ system,
137 a modified sequential gas delivery breathing circuit(13) was used to clamp $PETCO_2$ levels at the
138 desired +5 or -5 mmHg (depending on protocol). Breathing rate and tidal volumes were calibrated
139 prior to starting the breathing sequence.

MCA blood velocity and systemic blood pressure

141   While supine, continuous beat-to-beat arterial blood pressure was monitored using a Finapres®
142 Finometer system, where a finger cuff was placed on the middle phalange of the third finger, and
143 the finger blood pressure was calibrated with an upper arm cuff (Finapres® Medical Systems,
144 Amsterdam, Netherlands). The MCA was insonated with a 2 MHz ultrasound probe placed at the
145 temporal window and the peak blood flow velocity envelope was collected using the Neurovision
146 TCD System (Multigon Industries Inc., NY, USA). All analog data were sampled at 1000 Hz using
147 the PowerLab data acquisition system (ADInstruments, Dunedin, Otago, New Zealand).

MCA vascular diameter and blood velocity during MRI

149   A 7 Tesla MRI (Siemens, Magnetom Step 2.3, Erlangen, Germany) system was used to acquire
150 the following datasets: 1) 3D time-of-flight (TOF) with 0.8mm isotropic voxel resolution, echo
151 time (TE)/ repetition time (TR) = 2.59ms/18ms, flip angle (FA) = 15º, bandwidth (BW) =
152 203Hz/pxl; 2) single-slice 2D phase contrast (PC-MRI) for MCA M1 segment blood velocity, with
153 a voxel resolution of $0.3 \times 0.3 \times 1.4 mm^3$, TE/TR = 7.72ms/24.3ms, four averages, FA = 20º,
154 velocity-encoding (Venc) = 100cm/s and BW = 250Hz/pxl. During PC-MRI, a Venc value of

155 100cm/s was used for all subjects, except for one hypercapnic case, where a Venc of 130cm/s was
156 used to avoid wrap-around artifact; and 3) cross-sectional area of the MCA M1 segment using
157 single-slice 2D turbo spin-echo T1-weighted imaging with $0.5\times0.5\times1.5$ mm^3, TE/TR = 12/750ms,
158 BW = 270Hz/pxl, with an acquisition time of 13-14 seconds. The TOF data were used to locate a
159 straight segment on the right MCA M1 segment with the least curvature. The single-slice PC-MRI
160 and T1-weighted data were then acquired orthogonally to the axis of the selected MCA segment.
161 The T1-weighted data were acquired sequentially in order to monitor the changes in MCA
162 diameter.

Data analysis

164 Data analysis was carried out offline using custom R scripts (RStudio; v. 2020), GraphPad (V.8),
165 and LabChart Pro (v.8, ADInstruments, Dunedin, Otago, New Zealand).

Transcranial Doppler ultrasound

167 The MCA blood velocity (via TCD) and MAP were averaged beat-by-beat over the cardiac cycle
168 then were exported at 5 Hz sampling frequency and saved as text files (LabChart Pro v.8,
169 ADInstruments, Dunedin, Otago, New Zealand). During the TCD collection phase of testing, start
170 and end times of each event throughout the experimental breathing protocol were chronicled by
171 comments added in the LabChart file.

Magnetic resonance imaging (MRI; 7 Tesla)

173 During the MRI collection phase of testing, start and end times of each event were chronicled
174 based on the time associated with the desired PETCO$_2$ on the exported RespirAct™ data file. For
175 the T1-weighted anatomical MCA images, start and end times for each protocol event were
176 recorded based off the MRI console such that images were lined up offline based on the DICOM
177 image acquisition time. The brain anatomical images were imported into a DICOM reader, OsiriX
178 software (Pixmeo©, Bernex, Switzerland), and MCA cross-sectional area (CSA) was measured by
179 a blinded rater (MK) and compared against an expert rater (BKA).

180 The PC-MRI data were acquired for 30 seconds at baseline and within a ~70-second window
181 following 50-60 seconds from the start of steady-state hypercapnia (as noted on Fig 4, panel J with
182 the PC-MRI text bar). The MCA blood velocity measurements during the MRI session were
183 obtained from PC-MRI data by manually contouring a region-of-interest (ROI) inside the MCA

184   lumen. The contours were drawn using the software, signal processing in NMR (SPIN-Research,

185   MR Innovations Inc., Detroit, MI, USA). Care was taken to avoid any peripheral voxels within the

186   MCA lumen. The magnitude PC-MRI data was used to locate the MCA lumen. The peak velocities

187   were calculated for each subject for baseline and hypercapnic states.

Data extraction

189   The LabChart text files, the TCD and MRI session RespirAct™ breath-by-breath $PETCO_2$ values,

190   and the measured CSA were aligned using RStudio (v. 2020) (14) for data extraction from specific

191   epochs as indicated by the event comments in each file. The "print" function in the "magicfor"

192   package in R (15) was used to extract data with each loop iteration for each participant, and

193   variables of interest were exported as .csv files and imported to GraphPad Prism for graphing and

194   analysis.

195   Steady-state condition time courses were baseline corrected by subtracting mean baseline value (-

196   30 to 0 seconds of time window of interest) for each respective variable and plotted as delta values

197   (Fig. 4). For the baselines and steady-state condition, the data were extracted from the following

198   sections within the protocol: 1) 30 seconds baseline prior to onset of hypocapnia prior to the ramp

199   protocol and 2) 30 seconds baseline prior to steady-state hypercapnia, and 3) 60 seconds at the end

200   of steady-state hypercapnia. The ramp slope analysis included the entire hypocapnic to

201   hypercapnic incremental data (see below).

Ramp protocol

203   The target $PETCO_2$ and ramp protocol schematic is shown in Fig. 1, panel a. The target ventilation

204   rate was 12 breaths/minute and participants were coached using a visual metronome. In order to

205   equalize the spacing on the time axis when plotting the achieved $PETCO_2$ data, the $PETCO_2$ and

206   corresponding time vectors were resampled to a fixed 12 breaths/minute sampling rate using the

207   base R "approx" function in RStudio. Thus, two time vectors were created: 1) a target time vector

208   that is based off of a 12 breath/minute ventilation rate and 2) a "fixed" time vector that is based

209   off of resampling each participants data to meet the target time vector. The inter-individual

210   differences for the "fixed" time vector are indicated by horizontal error bars (mean ± S.D.; Fig. 3,

211   panels a-b), and the data are plotted and averaged for all participants along the target 12

212   breaths/minute time vector.

213 MCA blood velocity and systemic MAP data (in 0.2 second increments or 5 MHz sampling
214 frequency) were plotted from the hypocapnic state to the hypercapnic state during the ramp
215 protocol and averaged at each time point across the 12 participants (Fig. 3 panels c-d). Similarly,
216 the CSA values along the ramp protocol were averaged for each time point across participants
217 (Fig. 3 panel e). Although our goal was to collect 4 minutes of ramp data, the transition point from
218 the nadir of hypocapnia to start of ramp was different for each person and it generally took
219 approximately 2 breaths (~12 seconds) to sync with the desired $PETCO_2$ for the hypercapnic ramp.
220 Thus, to ensure the same number of samples (n=12) for each time point along the ramp protocol,
221 we only extracted the last 228 seconds of ramp data for all participants (instead of the full 240
222 seconds).

Steady-state protocol

224 Data extraction and organization were similar to the ramp protocol except data extraction occurred
225 between the start and end of the three-minute steady-state hypercapnia stimulus. As previously
226 mentioned, the PC-MRI data acquisition commenced 50-60 seconds from start of steady-state
227 hypercapnia. Thus, the continuous T1-anatomical MCA CSA scans were interrupted to allow for
228 PC-MRI imaging (correlation with TCD measures of blood velocity are shown in Fig. 2). PC-MRI
229 data were collected for 11 out of our 12 participants. As there were shifts in PC-MRI data collection
230 start and end times across participants, the upper and lower bounds of these time points are
231 indicated under the "PC-MRI" text bar on Fig. 3 (panel e, bottom row) to indicate to the reader
232 that the mean and S.D. for CSA values in this portion of the protocol do not include all 11
233 participants (i.e., n < 11) for the CSA data.

234 The averaged raw values for the 30 seconds baseline (prior to start of stead-state hypercapnia;
235 indicated as B on x-axis in Fig. 4) and last minute of steady-state hypercapnia (indicated as SSHC
236 on x-axis on Fig. 4) are shown in Fig. 4 for $PETCO_2$, MCA blood velocity (via TCD) and mean
237 arterial pressure (MAP) during the TCD session and the $PETCO_2$, MCA blood velocity (via PC-
238 MRI) and MCA CSA during the MRI session.

MCA blood velocity reactivity calculations

240 The ramp and steady-state hypercapnia MCA blood velocity cerebrovascular reactivity (CVR)
241 measures are shown in Fig. 5 panel a. For the ramp protocol, the MCA blood velocity slope (Fig.

242   3 panel c) and the PETCO$_2$ (for TCD session; Fig. 3 panel a) slope were calculated for each person

243   and the MCA blood velocity CVR was calculated as:

244    $$\text{MCA Blood Velocity CVR} = \frac{\text{MCA Blood Velocity Slope}}{\text{PETCO}_2 \text{ Slope}} \qquad (1)$$

245   For the steady-state hypercapnia protocol, the difference between the average baseline before start

246   of hypercapnia and the average of the last minute of hypercapnia (i.e., the difference between the

247   SSHC and B conditions in Fig. 4) were calculated. For each individual, the MCA blood velocity

248   CVR during the steady-state hypercapnia condition was then calculated as:

249    $$\text{MCA Blood Velocity CVR} = \frac{\Delta \text{MCA Blood Velocity}}{\Delta \text{PETCO}_2} \qquad (2)$$

250   *MCA blood flow reactivity calculations*

251   The ramp and steady-state hypercapnia MCA blood flow CVR measures are shown in Fig. 5 panel

252   b. For the ramp protocol, the MCA blood velocity was sectioned into 14 second averages

253   corresponding to each CSA image along the ramp protocol. Each of these averaged MCA blood

254   velocity values were multiplied by the corresponding CSA for the given time point to calculate

255   blood flow at 14 second increments along the ramp protocol. To keep it consistent with the MCA

256   blood velocity CVR measures, the PETCO$_2$ slopes from the TCD sessions were used as the

257   denominator during CVR calculations. The slopes were calculated for each person and the MCA

258   blood flow CVR was calculated for each individual as:

259    $$\text{MCA Blood Flow CVR} = \frac{\text{MCA Blood Flow Slope}}{\text{PETCO}_2 \text{ Slope}} \qquad (3)$$

260   Finally, to compare the MCA blood velocity CVR values and the MCA blood flow CVR values

261   calculated during the steady-state hypercapnia protocol, the percentage change from baseline for

262   each of the MCA blood velocity or blood flow were calculated (Fig. 5, panel c).

Statistical summary

264   Inter-rater variability was assessed using Bland-Altman analysis for 45 randomly selected images.

265   Pearson's correlation coefficient was used to test the correlation for inter-modality (TCD vs. PC-

266   MRI; Fig. 2) MCA blood velocity measures for both baseline and steady-state hypercapnia states

267   ($P < 0.05$ was considered to be statistically significant using a two-tailed test). In addition, linear

268   slope analysis was conducted to assess changes in PETCO$_2$, MAP, MCA CSA, and MCA blood

269   velocity variables during the ramp protocol. A probability level of $P<0.05$ indicates a non-zero

270   slope (the linear fits and p-values are labelled on Fig. 3 panels a-e). One-tailed paired t-tests were

271   conducted to compare variable responses during the steady-state hypercapnia condition versus

272   baseline (Fig. 4). Finally, to compare the MCA blood velocity CVR values and the MCA blood

273   flow CVR values calculated during the steady-state hypercapnia protocol, the percentage change

274   from baseline for each of the MCA blood velocity or blood flow was calculated (Fig. 5).

Results

276   Our CVR protocols with target $PETCO_2$ are illustrated in Fig. 1. Inter-rater variability for CSA

277   measures using the Bland-Altman test indicated a bias of 0.15 ± 0.26 mm^2 (mean ± S.D.; BKA -

278   MK) and 95% Limits of Agreement from -0.37 to 0.67 mm^2 (45 randomly selected images). Inter-

279   modality (TCD vs PC-MRI) correlation for MCA blood velocity measures indicated a significant

280   Pearson correlation between baseline and steady-state hypercapnia for each modality (n = 11

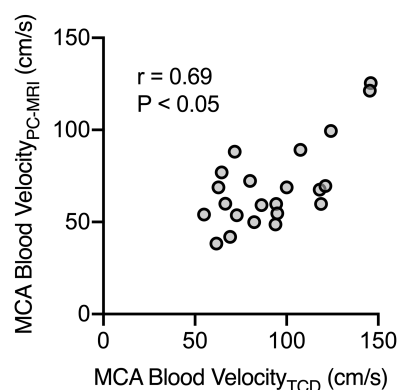281   participants, 22 pairs; r = 0.69, P < 0.05; Fig. 2).

Figure 2 – **MCA blood velocity measure comparison between TCD and PC-MRI**. Correlation plot comparing MCA blood velocity measured from transcranial Doppler (TCD) and phase contrast magnetic resonance imaging (PC-MRI). Baseline measures for both TCD and MRI sessions and steady-state hypercapnia measure at the ~1-2 minute mark for PC-MRI and in the last minute of steady-state hypercapnia for the TCD session for 22 pairs (n=11; r = 0.69, P<0.05).

282   Slope analysis during the ramp protocol indicated significant slopes (P<0.05; Fig. 3 panels a - d)

283   for achieved $\Delta PETCO_2$ (mmHg) during TCD (Y = 0.033*X – 3.96; $R^2 = 0.88$) and MRI (Y =

284   0.027*X – 2.54; $R^2 = 0.77$) sessions, with corresponding slopes for ΔMCA blood velocity (cm/s;

285   Y = 0.13*X – 13.70; $R^2 = 0.59$) and ΔMAP (mmHg; Y = 0.009*X – 0.38; $R^2 = 0.02$). Although

286   significant, the slope for MAP during the ramp protocol indicated an average <2mmHg increase

287   throughout the protocol. The slope of the MCA CSA with time did not show a deviation from 0

288   across the ramp protocol (Fig. 3, panel E; Y = 0.0008*X – 0.057; $R^2 = 0.006$).

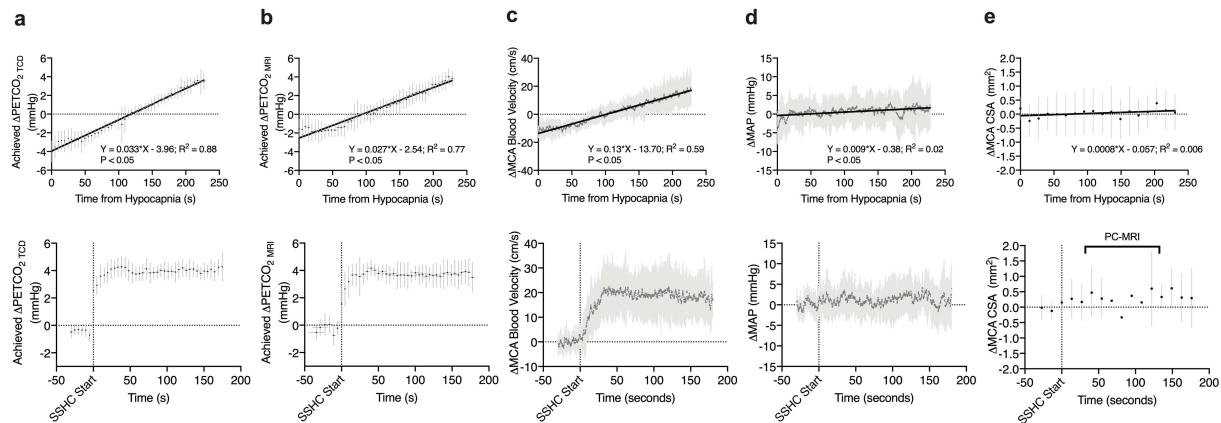Middle cerebral artery responses to vasoreactivity protocols

Figure 3 – Measured variables during the ramp and steady-state hypercapnia protocols. Ramp protocol (228 seconds; top row) responses and steady-state hypercapnia (180 seconds; bottom row) for delta changes in each variable from baseline levels are shown. Panel a: achieved $PETCO_2$ for TCD session, panel b: achieved $PETCO_2$ for MRI session, panel c: MCA blood velocity in TCD session, panel d: mean arterial pressure (MAP), and panel e: MCA cross-sectional area (CSA). The "PC-MRI" text on panel e bottom row indicates the variable time window in which PC-MRI images were acquired and there was an interruption in the consistent MCA CSA measurements. A 30 second baseline is shown for the steady-state hypercapnia condition (bottom row) and hypercapnia is indicated by SSHC on x-axis with a vertical line. Linear regressions (panels a-e top row) are shown for each variable in the ramp protocol and a significant (non-zero; α level significance 0.05) slope is indicated by $P < 0.05$. N = 12 for all variables with data presented as mean±S.D.

289 During the steady-state hypercapnia protocol, $PETCO_2$ increased during steady-state hypercapnia

290 from baseline with a mean difference of 4.45 mmHg and 95% CI of 4.05 to 4.85 when using TCD

291 (44.3±3.1 vs. 39.9±2.9 mmHg, respectively; n=12, η_p^2=0.98, P<0.05; Fig. 4, panel a) and a mean

292 difference of 3.75 and 95% CI of 3.29 to 4.20 when using MRI (42.7±4.2 vs. 38.9±4.4 mmHg,

293 respectively; n=12, η_p^2=0.97, P<0.05; Fig. 4, panel b) sessions. Similarly, MCA blood velocity

294 increased with steady-state hypercapnia from baseline with a mean difference of 18 cm/s and 95%

295 CI of 13 to 24 cm/s in the TCD trial (104±29 vs. 86±24 cm/s, respectively; n=12, η_p^2=0.83, P<0.05;

296 Fig. 4, panel c) and a mean difference of 22 cm/s and 95% CI of 12 to 33 when using MRI (via

297 PC-MRI; 79±15 vs. 59±9 cm/s, respectively; n=11, η_p^2=0.70, P<0.05; Fig. 4 panel e) sessions, and

298 MCA CSA increased with a mean difference of 0.31 mm^2 and 95% CI of -0.03 to 0.66 mm^2 during

299 the MRI session (5.71±1.03 vs. 5.34±0.97 mm^2, respectively; n=12, η_p^2=0.27, P<0.05; Fig. 4,

300 panel f). The mean difference in MAP between the last minute of steady-state hypercapnia and

301 baseline was 1.35 mmHg with a 95% CI of -0.82 to 3.5 mmHg which is most compatible with a

302 negligible change (90±8 vs. 89±8 mmHg, respectively; n=12; η_p^2=0.14, Fig. 4, panel e). Calculated

303 MCA blood flows (product of MCA blood velocity and CSA) increased from baseline to steady-

304 state hypercapnia (267±54 vs. 348±78 ml/min, respectively; P<0.05, one-tailed paired t-test) with

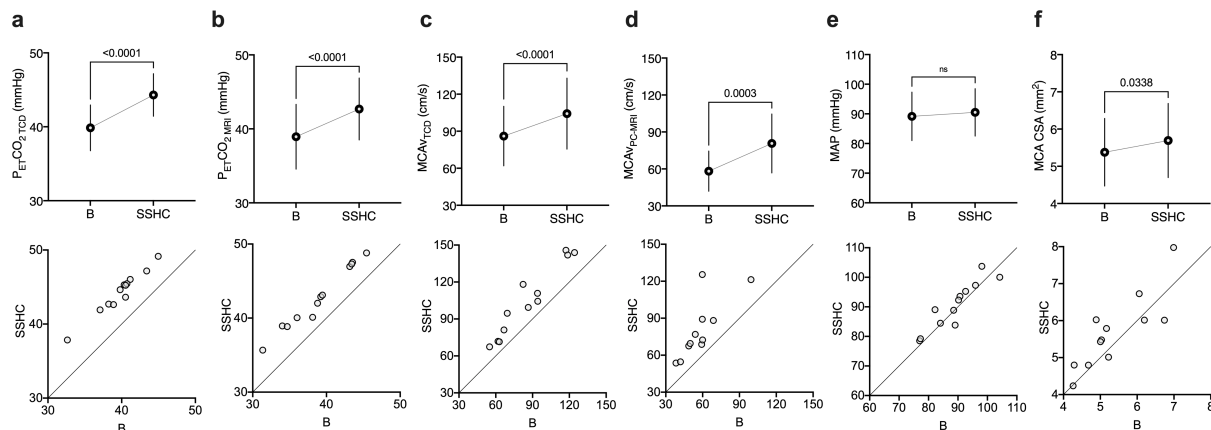305 a delta calculated blood flow of 81±30 ml/min.

Figure 4 – Baseline (B) and steady-state hypercapnia (SSHC) comparisons. Top row: Baseline (B) and steady-state hypercapnia (SSHC) measures (n=12 except for panel d where n=11, mean±S.D.). Where statistical significance occurs, p-values are indicated above data (ns = not significant; paired t-test; α level significance 0.05). Bottom row: Individual data points (n=12 except for panel d where n=11) comparing baseline (B) to steady-state hypercapnia (SSHC) responses for the same variable in that column as top row. The diagonal line (identity line) indicates where data would fall if there was no measurable effect of SSHC from B. Data above the identity line indicates an increase in variable measure with SSHC (from baseline; B).

306

307 The mean difference in MCA blood velocity-based measure of CVR between the ramp and steady-

308 state hypercapnia protocols was 0.18 with 95% CI of -0.59 to 0.96 which is most compatible with

309 a negligible effect of protocol on MCA blood velocity CVR (3.8±1.7 vs. 4.0±1.6 cm/s/mmHg,

310 respectively; n=12, two-tailed paired t-test, p=0.62, η_p^2=0.02, Fig. 5, panel a). The mean difference

311 in calculated MCA blood flow-based measure of CVR between the steady-state protocol and ramp

312 protocol was 5.0 with a 95% CI of 2.8 to 7.2 ml/min/mmHg and was statistically significant

313 (17.3±5.7 vs. 12.3±4.5 ml/min/mmHg, respectively; n=12, two-tailed t-test, P<0.05, η_p^2=0.70,

314 two-tailed t-test; Fig. 5, panel b). Similarly, when calculated as %change in MCA blood velocity

315 or MCA blood flow over the ΔPETCO$_2$ during hypercapnia, the mean difference between MCA

316 blood flow CVR and MCA blood velocity CVR was (6.7±1.6 vs. 4.8±2.0 %/mmHg, respectively;

317 n = 12, P<0.05, one-tailed t-test). Finally, the %change of MCA blood flow was greater than the

318 %change of MCA blood velocity during the steady-state condition with a mean difference of 6.9

319 and 95% CI of -0.37 to 14.10 (29.8±8.2 vs. 21.5±9.6 %, respectively; n=12, P<0.05, one-tailed t-

320 test; Fig. 5, panel c).

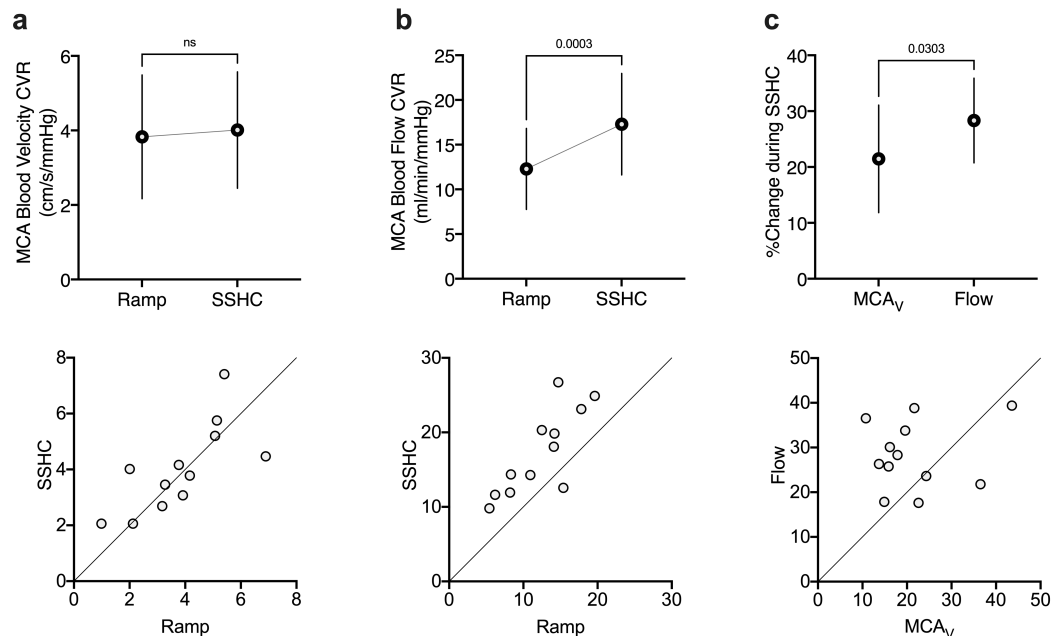Middle cerebral artery responses to vasoreactivity protocols

Figure 5 – Middle cerebral artery (MCA) blood velocity and flow reactivity across protocols
Top row: Calculated MCA blood velocity cerebrovascular reactivity (CVR) was not different between ramp and steady-state hypercapnia (SSHC; panel a), while MCA blood flow CVR was higher in SSHC compared to the ramp protocol (panel b). The percent change in calculated MCA blood flow from baseline was higher than the percent change in MCA blood velocity from baseline (panel c) with SSHC. Where statistical significance occurs, p-values are indicated above data (ns = not significant; paired t-test; α level significance 0.05). N=12 for all variables with data presented as mean±S.D. Bottom row: Individual data points (n=12) comparing ramp to steady-state hypercapnia (SSHC) responses (panels a-b) for the same variable in that column as top row or MCA blood velocity to calculated MCA blood flow (panel c). The diagonal line (identity line) indicates where data would fall if there was no measurable effect of protocol on CVR measures (panels a-b) or effect of accounting for MCA CSA in flow calculations (compared to using MCAv alone as an index of flow) when assessing %change of flow or MCAv during SSHC (panel c). Data above the identity line indicates an increase in variable measure with SSHC (compared to ramp; panels a-b) or higher %change in flow value for a given %change in MCAv.

Discussion

321   This is the first study to provide MCA CSA measures across ramp and steady-state hypercapnia

322   protocols, enabled by the ability to obtain MCA CSA measurements every 14 seconds with

323   prospective targeting of PETCO$_2$. This approach enabled direct comparisons of the steady- state

324   versus a ramp protocols to establish valid CVR calculations using only measures of flow velocity.

325   The noteworthy findings of this study are that: 1) the MCA CSA did not change during the ramp

326   protocol with delta ~ -3 to +4 mmHg of PETCO$_2$, but did increase with steady-state hypercapnia

328   ~ +4 mmHg of PETCO$_2$), 2) blood pressure remained stable throughout duration of both ramp and

329   steady-state protocols, and 3) CVR measures based on MCA blood velocity cerebrovascular

330   reactivity was not different between ramp and steady-state protocols, but 4) MCA blood flow-

331   based CVR was greater during steady-state compared to the ramp protocol. Taken together, the

332   ramp protocol seems to result in similar CVR values as those observed in the steady-state protocol,

333   with the added advantage of having minimal and negligible effects on MCA CSA or MAP in the

334   face of moderate elevations in PETCO$_2$.

335   ***Transcranial Doppler – MCA blood velocity & CVR measures***

336   Often, CVR is characterized by the slope in the linear relationship between MCA blood velocity

337   and PETCO$_2$ with respect to each variable's relative change with time. The relationship between

338   arterial blood velocity and CO$_2$ (16) is sigmoidal and both the range and starting point of PETCO$_2$

339   affect the arterial blood velocity response to CO$_2$ (17). Regan *et al*. (7) showed a lower MCA blood

340   velocity-based CVR during steady-state hypercapnia (ΔPETCO$_2$ of 10 mmHg) than during the

341   ramp hypercapnic protocol (-5 to +10 mmHg PETCO$_2$). However, these ranges of PETCO$_2$ can

342   elicit systemic hemodynamic effects (6) that can increase blood velocity changes independent of

343   cerebral vascular bed dilation. The current protocols used a lower dose of change in PETCO$_2$ in

344   order to avoid the central hemodynamic and non-linear portions of the CVR curve.

345   ***MRI – MCA CSA & CVR measures***

346   In the current study, PETCO$_2$ values at the ends of both ramp and steady-state hypercapnia

347   protocols, and the calculated MCA blood velocity CVR measures, were not different between the

348   two protocols. Yet, the PETCO$_2$ changes during the ramp protocol did not affect MCA CSA in

349   same the way that the steady-state hypercapnia protocol did. To quantify transient MCA CSA

350   measures, we developed an anatomical scan optimized to provide MCA images every 14 seconds.

351   This enabled imaging of the MCA during the dynamic stimuli such as the ramp protocol or onset

352   of the steady state protocol, as well as improving temporal sensitivity during the steady-state

353   model. To our knowledge, our 14 second anatomical scan of MCA CSA provides the highest level

354   of temporal resolution (i.e., shortest acquisition time) available when compared to existing

355   assessments of MCA CSA during steady-state hypercapnia protocols. From our current MCA CSA

356   findings, the MCA dilates under conditions where hypercapnia is elevated and sustained (i.e.

357   steady-state hypercapnia), rather than with brief exposure to elevated levels of PETCO$_2$ (i.e., end

358   of ramp protocol). This observation is supported by previous studies indicating a slow onset to

359   dilation in either the internal carotid artery (18) or the MCA (2), despite immediate changes in

360   MCA blood velocity that reflect downstream microvascular dilation to early hypercapnia.

361   This study supports previous MCA CSA findings in CVR studies that indicate MCA CSA dilates

362   after ~2 minutes of steady-state hypercapnia using 3T (2) and 7T MRI (4,5). Thus, CVR values

363   during the steady-state protocol indicated significant error when the MCA cross-sectional area was

364   not included. Specifically, we found that the %change in MCA blood velocity was lower than the

365   %change in MCA blood flow by ~7% (mean difference between these two measures). This value

366   is less than the 18% observed in work by Coverdale et al. (2). We believe the discrepancy in these

367   mean differences is due to the magnitude of hypercapnia achieved in each study, with ~ $+\Delta4$ mmHg

368   $PETCO_2$ in the current study versus ~ $+\Delta10$ mmHg in $PETCO_2$ for the study by Coverdale et al.

369   As well, there was a 5% increase in MAP in the study by Coverdale et al. (~4 mmHg) which was

370   greater than the increase in MAP for our study (~2 mmHg for ramp, and ~1 mmHg for steady-

371   state), a difference that may be attributed to the greater magnitude of the hypercapnia stimulus in

372   the the previous study. While mild variations in MAP are accounted for by autoregulatory

373   mechanisms such that MCA blood flow is sustained with negligible influence on MCA CSA,

374   autoregulation mechanisms are impaired during hypercapnia (19). Thus, we anticipate that the

375   higher the hypercapnic magnitude, the greater the risk that MAP will influence MCA CSA (and/or

376   blood velocity) augmenting any discrepancies between MCA blood velocity and calculated MCA

377   blood flow.

378   This is the first study to use a sequential gas delivery circuit (via the RespirAct™) when assessing

379   MCA CSA responses during hypercapnia, thereby more closely aligning partial pressure of arterial

380   and end-tidal CO_2 levels (20). Interestingly, we achieved similar MCA blood flow CVR during

381   steady-state hypercapnia as previous work (2), and our MCA blood velocity CVR for both the

382   steady-state hypercapnia (2,21) and ramp protocol (7) were in agreement with previous studies.

383   As recommended by Regan et al. (7), when using a limited range of $PETCO_2$ values during a

384   hypercapnic protocol, a linear approach to CVR analysis is appropriate.

385   Everything considered, a CVR measure based solely on TCD-acquired MCA blood velocity

386   measures during a ramp hypercapnia protocol seems to elicit a similar CVR outcome as the

387   commonly used steady-state protocol, but without the limitation of potential changes in MCA

388   CSA. CVR outcome measures involve calculating MCA blood velocity changes for a given change

389   in $PETCO_2$. Similarly, our study illustrates that even modest values of change in $PETCO_2$ achieve

390   a comparable value of CVR at higher hypercapnic doses.

Methodological Considerations

392   Our overall target range for manipulating $PETCO_2$ during the cerebrovascular reactivity was

393   between the $-\Delta5$ to $+\Delta5$ from baseline $PETCO_2$ (10). While our findings support a lack of MCA

394   CSA changes during ramp protocols of $-\Delta3$ to $+\Delta4$ mmHg in $PETCO_2$, we cannot make conclusive

395   remarks on MCA CSA changes during a ramp protocol of $\pm\Delta5$mmHg in $PETCO_2$. However, as

396   mentioned above, our values of $\Delta PETCO_2$ fell within our target $\pm\Delta5$mmHg from baseline $PETCO_2$

397   range, the CVR measures are consistent with previous studies where higher levels of $PETCO_2$

398   were used, and we found negligible increases in MAP. Therefore, the modest level of $PETCO_2$

399   achieved here appear to have achieved the major objectives. The ramp protocol designed for the

400   current study also achieved an optimal balance between stimulus and central hemodynamics. We

401   acknowledge however, that we did not account for the impact of the ~2 mmHg rise in MAP during

402   the ramp protocol, which we expect to be negligible in impacting MCA CSA.

403   Although we were unable to measure continuous blood pressure and MCA blood velocity during

404   the MRI trial, we measured blood velocity data during the MRI session via the PC-MRI sequence.

405   Testing of the TCD and MRI segments of the study were collected consecutively within a 2-hour

406   window with the order of tests varied across participants. The absolute values for MCA blood

407   velocities measured by PC-MRI were lower than our TCD measures, although we suspect this had

408   to do with our pre-set Venc value choice of 100 cm/s which may have cut off some of the higher

409   velocities. Our rationale for not choosing a higher Venc than 100 cm/s was the possibility of cutting

410   off lower velocity values during baseline. Regardless, the increase in MCA blood velocity during

411   hypercapnia (from baseline) were in agreement between the two techniques (TCD: $\sim\Delta18$ cm/s and

412   PC-MRI: $\sim\Delta20$ cm/s). Thus, we assume that the blood pressure responses during the TCD and

413   MRI sessions were similar as well.

414   Finally, the current results are delimited to young healthy adults Thus, additional studies are

415   needed to understand the effects of age, a group that demonstrates greater MAP responses to

416   hypercapnia and variable responses in CSA changes (9), or other differentiating conditions.

417 Further, our study was conducted in the supine position, which is less replicable for CVR studies
418 than the seated position (22) and may explain some of the disparity of blood velocity measures for
419 some individuals between the two protocols: the supine posture is necessary for MRI studies.
420 Additional studies are required to address the impact of CSA changes and protocol model on
421 posture-dependent intra-subject variability so that reliable CVR protocols can be used to make
422 inferences on vascular health (e.g., inferred vascular dysfunction with reduced CVR). The current
423 data suggest that the ramp protocol might be useful in reducing inter-study variability.

Conclusions

425 A constant CSA during experimental vasoreactive challenges is essential to the reliability of TCD-
426 acquired blood velocity as a correlative index of blood flow changes. In this study, we showed
427 data that were most compatible with negligible change in MCA CSA from baseline during a graded
428 ramp hypercapnic protocol ($\pm \sim\Delta 4$ mmHg from baseline $PETCO_2$). Similar to our previous work,
429 the MCA data align best with an interpretation of MCA dilation during a prolonged (3-minutes)
430 $\sim\Delta 4$ mmHg in baseline $PETCO_2$ period of hypercapnia, and confirmed the expected error in
431 %change of MCA blood velocity as an index of blood flow and in the calculated CVR when a
432 change in CSA is not considered (2). Combined, these data suggest that during transient changes
433 in $PETCO_2$, as in the ramp protocol, the constant segment of the sigmoid may describe MCA CSA
434 changes with $PETCO_2$, and any changes in blood velocity can reflect CBF. In summary, the ramp
435 protocol with $\pm \sim\Delta 4$ mmHg from baseline $PETCO_2$ appears to provide expected measures of CVR
436 where blood velocity should reflect blood flow patterns of change.

Acknowledgements

Author contribution statement

444

445 BKA conceptualized and designed the study, collected, analyzed, and disseminated the data, and
446 wrote and edited the manuscript. SB assisted with study design, data collection and analysis, and
447 assisted with writing and editing the manuscript. MK assisted with data collection, analysis and
448 interpretation and editing of the manuscript. BJM assisted with data collection, organization, and
449 editing the manuscript. KN assisted with study design and editing of the manuscript. RSM assisted
450 with study design and editing of the manuscript. JKS conceptualized and designed the study, and
451 assisted with data dissemination, writing and editing of the manuscript.

Conflict of interest

452

453 The authors do not have any conflicts of interest to disclose.

454

455

456

457

458

459

460

References

461

462   1. Portegies MLP, de Bruijn RFAG, Hofman A, Koudstaal PJ, Ikram MA. Cerebral vasomotor
463   reactivity and risk of mortality: the Rotterdam Study. Stroke. 2014 Jan;45(1):42–7.

464   2. Coverdale NS, Gati JS, Opalevych O, Perrotta A, Shoemaker JK. Cerebral blood flow
465   velocity underestimates cerebral blood flow during modest hypercapnia and hypocapnia. J
466   Appl Physiol Bethesda Md 1985. 2014 Nov 15;117(10):1090–6.

467   3. Howe CA, Caldwell HG, Carr J, Nowak-Flück D, Ainslie PN, Hoiland RL. Cerebrovascular
468   reactivity to carbon dioxide is not influenced by variability in the ventilatory sensitivity to
469   carbon dioxide. Exp Physiol. 2020;105(5):904–15.

470   4. Al-Khazraji BK, Shoemaker LN, Gati JS, Szekeres T, Shoemaker JK. Reactivity of larger
471   intracranial arteries using 7 T MRI in young adults. J Cereb Blood Flow Metab Off J Int Soc
472   Cereb Blood Flow Metab. 2019 Jul;39(7):1204–14.

473   5. Verbree J, Bronzwaer A-SGT, Ghariq E, Versluis MJ, Daemen MJAP, van Buchem MA, et
474   al. Assessment of middle cerebral artery diameter during hypocapnia and hypercapnia in
475   humans using ultra-high-field MRI. J Appl Physiol Bethesda Md 1985. 2014 Nov
476   15;117(10):1084–9.

477   6. Shoemaker JK, Vovk A, Cunningham DA. Peripheral chemoreceptor contributions to
478   sympathetic and cardiovascular responses during hypercapnia. Can J Physiol Pharmacol.
479   2002 Dec;80(12):1136–44.

480   7. Regan RE, Fisher JA, Duffin J. Factors affecting the determination of cerebrovascular
481   reactivity. Brain Behav. 2014 Sep;4(5):775–88.

482   8. Stefanidis KB, Askew CD, Klein T, Lagopoulos J, Summers MJ. Healthy aging affects
483   cerebrovascular reactivity and pressure-flow responses, but not neurovascular coupling: A
484   cross-sectional study. PLOS ONE. 2019 May 16;14(5):e0217082.

485   9. Coverdale NS, Badrov MB, Shoemaker JK. Impact of age on cerebrovascular dilation versus
486   reactivity to hypercapnia. J Cereb Blood Flow Metab. 2017 Jan 1;37(1):344–55.

487   10. Hoiland RL, Fisher JA, Ainslie PN. Regulation of the Cerebral Circulation by Arterial
488   Carbon Dioxide. Compr Physiol. 2019 Jun 12;9(3):1101–54.

489   11. McKetton L, Cohn M, Tang-Wai DF, Sobczyk O, Duffin J, Holmes KR, et al.
490   Cerebrovascular Resistance in Healthy Aging and Mild Cognitive Impairment. Front Aging
491   Neurosci. 2019;11:79.

492   12. Fisher JA, Sobczyk O, Crawley A, Poublanc J, Dufort P, Venkatraghavan L, et al. Assessing
493   cerebrovascular reactivity by the pattern of response to progressive hypercapnia. Hum Brain
494   Mapp. 2017 Jul;38(7):3415–27.

495 13. Brothers RM, Lucas RAI, Zhu Y-S, Crandall CG, Zhang R. Cerebral vasomotor reactivity:
496   steady-state versus transient changes in carbon dioxide tension. Exp Physiol. 2014
497   Nov;99(11):1499–510.

498 14. Core Team R. R: A language and environment for statistical computing. R Foundation for
499   Statistical Computing, Vienna, Austria (2013). Suppl Fig S. 2015;2.

500 15. Makiyama K. magicfor: Magic Functions to Obtain Results from for Loops [Internet]. 2016
501   [cited 2021 Jan 9]. Available from: https://CRAN.R-project.org/package=magicfor

502 16. Battisti-Charbonney A, Fisher J, Duffin J. The cerebrovascular response to carbon dioxide in
503   humans. J Physiol. 2011 Jun 15;589(Pt 12):3039–48.

504 17. Sobczyk O, Battisti-Charbonney A, Fierstra J, Mandell DM, Poublanc J, Crawley AP, et al.
505   A conceptual model for CO_2-induced redistribution of cerebral blood flow with experimental
506   confirmation using BOLD MRI. NeuroImage. 2014 May 15;92:56–68.

507 18. Willie CK, Macleod DB, Shaw AD, Smith KJ, Tzeng YC, Eves ND, et al. Regional brain
508   blood flow in man during acute changes in arterial blood gases. J Physiol. 2012 Jul
509   15;590(14):3261–75.

510 19. Panerai RB, Deverson ST, Mahony P, Hayes P, Evans DH. Effects of CO2 on dynamic
511   cerebral autoregulation measurement. Physiol Meas. 1999 Aug;20(3):265–75.

512 20. Ito S, Mardimae A, Han J, Duffin J, Wells G, Fedorko L, et al. Non-invasive prospective
513   targeting of arterial P(CO2) in subjects at rest. J Physiol. 2008 Aug 1;586(15):3675–82.

514 21. Burley CV, Lucas RAI, Whittaker AC, Mullinger K, Lucas SJE. The CO2 stimulus duration
515   and steady-state time point used for data extraction alters the cerebrovascular reactivity
516   outcome measure. Exp Physiol. 2020 May;105(5):893–903.

517 22. McDonnell MN, Berry NM, Cutting MA, Keage HA, Buckley JD, Howe PRC. Transcranial
518   Doppler ultrasound to assess cerebrovascular reactivity: reliability, reproducibility and effect
519   of posture. PeerJ. 2013 Apr 9;1:e65.

520